Electronic Supplementary Material (ESI) for Soft Matter.

Supplementary Information

Structural and Dynamic Heterogeneity in Associative Networks Formed by Artificially Engineered Protein Polymers

Ameya Rao[1] and Bradley D. Olsen[1]*

[1]Department of Chemical Engineering, Massachusetts Institute of Technology, Cambridge, MA 02139

*Corresponding Author
Bradley D. Olsen
Tel: (617) 715-4548
Email: bdolsen@mit.edu

Table of Contents

1. Amino acid sequences of artificial proteins

Amino acids in red comprise the coiled-coil P domains, while amino acids in blue comprise the random coil C_x domains. Cysteine residues are in green.

$PC_{10}P$:

MRGSHHHHHHGSGDLAPQMLRELQETNAALQDVRELLRQQVKEITFLKNTVMESDAS
GTSYRDPMGAGAGAGPEGAGAGAGPEGAGAGAGPEGAGAGAGPEGAGAGAGPEGAG
AGAGPEGAGAGAGPEGAGAGAGPEGAGAGAGPEGAGAGAGPEGARMPTSGSGDL
APQMLRELQETNAALQDVRELLRQQVKE ITFLKNTVMESDASGKLN

$PC_{30}P$:

MRGSHHHHHHGSGDLAPQMLRELQETNAALQDVRELLRQQVKEITFLKNTVMESDAS
GTSYRDPMGAGAGAGPEGAGAGAGPEGAGAGAGPEGAGAGAGPEGAGAGAGPEGAG
AGAGPEGAGAGAGPEGAGAGAGPEGAGAGAGPEGAGAGAGPEGARMPTSYRDPMGA
GAGAGPEGAGAGAGPEGAGAGAGPEGAGAGAGPEGAGAGAGPEGAGAGAGPEGAGA
GAGPEGAGAGAGPEGAGAGAGPEGAGAGAGPEGARMPTSYRDPMGAGAGAGPEGAG
AGAGPEGAGAGAGPEGAGAGAGPEGAGAGAGPEGAGAGAGPEGAGAGAGPEGAGAG
AGPEGAGAGAGPEGAGAGAGPEGARMPTSGSGDLAPQMLRELQETNAALQDVRELLR
QQVKEITFLKNTVMESDASGKLN

$C_{10}(PC_{10})_4$:

MRGSHHHHHHGSDDDDKASYRDPMGAGAGAGPEGAGAGAGPEGAGAGAGPEGAGA
GAGPEGAGAGAGPEGAGAGAGPEGAGAGAGPEGAGAGAGPEGAGAGAGPEGAGAGA
GPEGARMPTSAPQMLRELQETNAALQDVRELLRQQVKEITFLKNTVMESDASGTSYRD
PMGAGAGAGPEGAGAGAGPEGAGAGAGPEGAGAGAGPEGAGAGAGPEGAGAGAGPE
GAGAGAGPEGAGAGAGPEGAGAGAGPEGAGAGAGPEGARMPTSAPQMLRELQETNA
ALQDVRELLRQQVKEITFLKNTVMESDASGTSYRDPMGAGAGAGPEGAGAGAGPEGA
GAGAGPEGAGAGAGPEGAGAGAGPEGAGAGAGPEGAGAGAGPEGAGAGAGPEGAGA
GAGPEGAGAGAGPEGARMPTSAPQMLRELQETNAALQDVRELLRQQVKEITFLKNTVM
ESDASGTSYRDPMGAGAGAGPEGAGAGAGPEGAGAGAGPEGAGAGAGPEGAGAGAG
PEGAGAGAGPEGAGAGAGPEGAGAGAGPEGAGAGAGPEGAGAGAGPEGARMPTSAP
QMLRELQETNAALQDVRELLRQQVKEITFLKNTVMESDASGTSYRDPMGAGAGAGPEG
AGAGAGPEGAGAGAGPEGAGAGAGPEGAGAGAGPEGAGAGAGPEGAGAGAGPEGAG
AGAGPEGAGAGAGPEGAGAGAGPEGARMPTSW

PC_5-cys-C_5P:

MRGSHHHHHHGSGDLAPQMLRELQETNAALQDVRELLRQQVKEITFLKNTVMESDAS
GTSYRDPMGAGAGAGPEGAGAGAGPEGAGAGAGPEGAGAGAGPEGAGAGAGPEGCA
GAGAGPEGAGAGAGPEGAGAGAGPEGAGAGAGPEGAGAGAGPEGARMPTSGSGDLA
PQMLRELQETNAALQDVRELLRQQVKEITFLKNTVMESDASGKLN

PC_5-cys-$C_{25}P$:

MRGSHHHHHHGSGDLAPQMLRELQETNAALQDVRELLRQQVKEITFLKNTVMESDAS
GTSYRDPMGAGAGAGPEGAGAGAGPEGAGAGAGPEGAGAGAGPEGAGAGAGPEGCA
GAGAGPEGAGAGAGPEGAGAGAGPEGAGAGAGPEGAGAGAGPEGARMPTSYRDPMG
AGAGAGPEGAGAGAGPEGAGAGAGPEGAGAGAGPEGAGAGAGPEGAGAGAGPEGAG
AGAGPEGAGAGAGPEGAGAGAGPEGAGAGAGPEGARMPTSYRDPMGAGAGAGPEGA
GAGAGPEGAGAGAGPEGAGAGAGPEGAGAGAGPEGAGAGAGPEGAGAGAGPEGAGA
GAGPEGAGAGAGPEGAGAGAGPEGARMPTSGSGDLAPQMLRELQETNAALQDVRELL
RQQVKEITFLKNTVMESDASGKLN

$C_{10}(PC_{10})_4$-cys:

MRGSHHHHHHGSDDDDKTSYRDPMGAGAGAGPEGAGAGAGPEGAGAGAGPEGAGA
GAGPEGAGAGAGPEGAGAGAGPEGAGAGAGPEGAGAGAGPEGAGAGAGPEGAGAGA
GPEGARMPTSAPQMLRELQETNAALQDVRELLRQQVKEITFLKNTVMESDASGTSYRD
PMGAGAGAGPEGAGAGAGPEGAGAGAGPEGAGAGAGPEGAGAGAGPEGAGAGAGPE
GAGAGAGPEGAGAGAGPEGAGAGAGPEGAGAGAGPEGARMPTSAPQMLRELQETNA
ALQDVRELLRQQVKEITFLKNTVMESDASGTSYRDPMGAGAGAGPEGAGAGAGPEGA
GAGAGPEGAGAGAGPEGAGAGAGPEGAGAGAGPEGAGAGAGPEGAGAGAGPEGAGA
GAGPEGAGAGAGPEGARMPTSAPQMLRELQETNAALQDVRELLRQQVKEITFLKNTVM
ESDASGTSYRDPMGAGAGAGPEGAGAGAGPEGAGAGAGPEGAGAGAGPEGAGAGAG
PEGAGAGAGPEGAGAGAGPEGAGAGAGPEGAGAGAGPEGAGAGAGPEGARMPTSAP
QMLRELQETNAALQDVRELLRQQVKEITFLKNTVMESDASGTSYRDPMGAGAGAGPEG
AGAGAGPEGAGAGAGPEGAGAGAGPEGAGAGAGPEGAGAGAGPEGAGAGAGPEGAG
AGAGPEGAGAGAGPEGAGAGAGPEGARMPTSCKLNS

C_5PC_5-cys:

MRGSHHHHHHGSCASAGAGAGPEGAGAGAGPEGAGAGAGPEGAGAGAGPEGAGAGA
GPEGARMPTSAPQMLRELQETNAALQDVRELLRQQVKEITFLKNTVMESDASGTSYRD
PMGAGAGAGPEGAGAGAGPEGAGAGAGPEGAGAGAGPEGAGAGAGPEGTSDDDDKR
SHHHHHH

2. Neutron scattering patterns and fit parameters for all gels

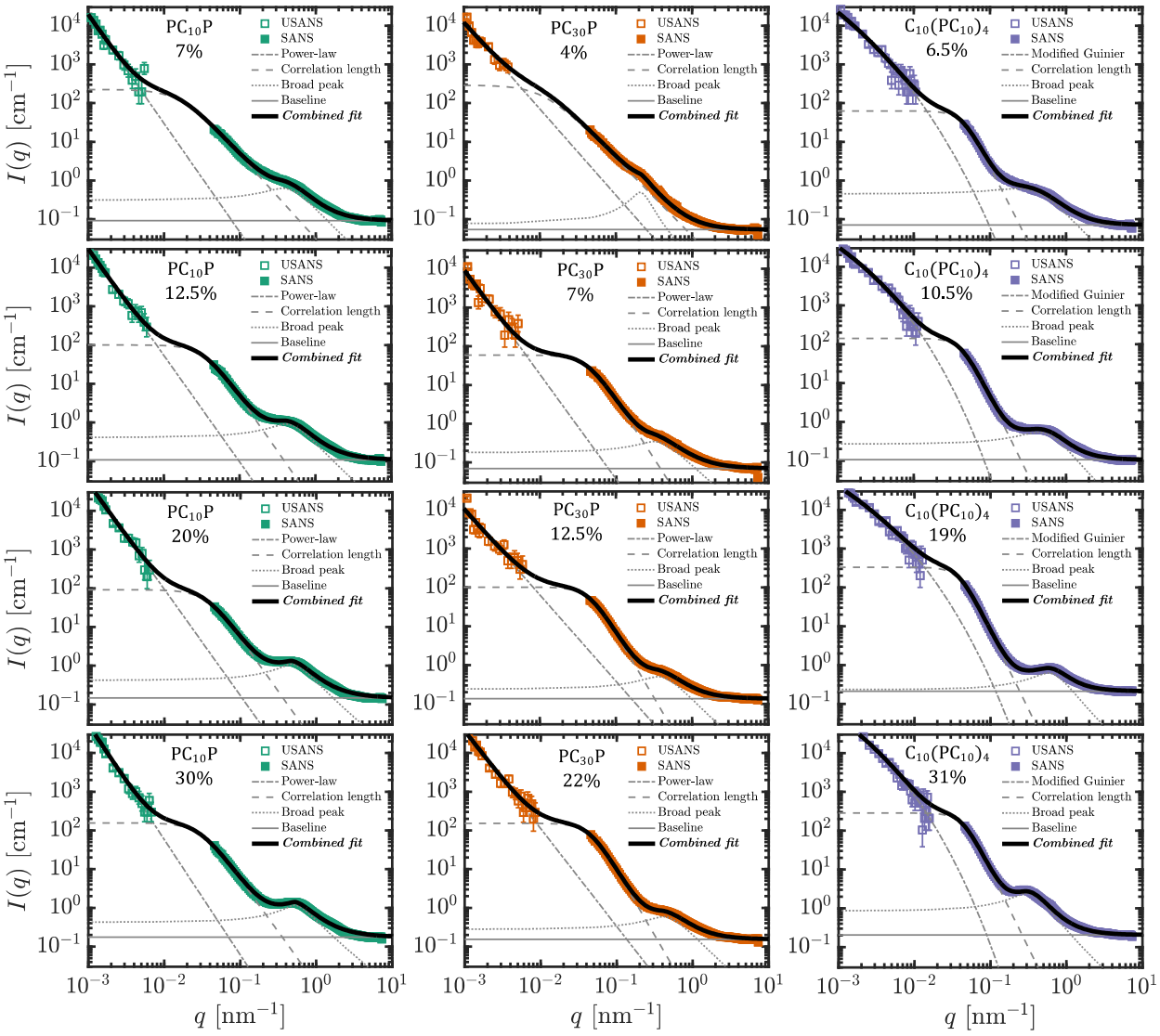

Figure S1. Combined SANS and USANS patterns for all protein gels collected at 25 ˚C fit to the double-correlation-length model (Eq. 4 in the main text) with fit components provided in gray.

Table S1. Neutron scattering fit parameters for all protein gels measured at 25 ˚C from fits to the double-correlation-length model (Equation 4 in the main text). Uncertainties are standard deviations of fits to 100 bootstrapped replicas of each scattering pattern, as described in Ref.[1] Concentrations were chosen to match junction densities across different protein gels.

$PC_{10}P$

	7%	**12.5%**	**20%**	**30%**
A	$(1 \pm 3) \times 10^{-7}$	$(5 \pm 7) \times 10^{-7}$	$(6 \pm 7) \times 10^{-7}$	$(1 \pm 1) \times 10^{-7}$
n	3.0 ± 0.3	2.8 ± 0.2	2.8 ± 0.2	3.0 ± 0.2
$B\ [cm^{-1}]$	220 ± 60	100 ± 20	100 ± 30	150 ± 20
$\Xi\ [nm]$	59 ± 9	30 ± 3	28 ± 4	34 ± 2
m_1	2.18 ± 0.05	2.81 ± 0.06	2.77 ± 0.06	2.73 ± 0.04
$C\ [cm^{-1}]$	0.64 ± 0.02	0.920 ± 0.007	1.112 ± 0.006	1.189 ± 0.003
$q_0\ [nm^{-1}]$	0.369 ± 0.006	0.413 ± 0.004	0.475 ± 0.003	0.526 ± 0.002
$\xi\ [nm]$	2.71 ± 0.02	2.72 ± 0.02	2.88 ± 0.03	2.80 ± 0.02
m_2	1.70 ± 0.01	1.64 ± 0.01	1.54 ± 0.01	1.468 ± 0.007
$D\ [cm^{-1}]$	0.0919 ± 0.0003	0.1087 ± 0.0003	0.1466 ± 0.0004	0.1739 ± 0.0005

$PC_{30}P$

	4%	**7%**	**12.5%**	**22%**
A	$(6 \pm 10) \times 10^{-5}$	$(1 \pm 5) \times 10^{-5}$	$(3 \pm 6) \times 10^{-5}$	$(3 \pm 4) \times 10^{-6}$
n	2.2 ± 0.2	2.6 ± 0.3	2.3 ± 0.3	2.6 ± 0.2
$B\ [cm^{-1}]$	300 ± 100	60 ± 10	100 ± 10	150 ± 10
$\Xi\ [nm]$	90 ± 20	24 ± 2	23 ± 1	22.7 ± 0.6
m_1	2.03 ± 0.06	3.1 ± 0.1	3.3 ± 0.1	3.38 ± 0.04
$C\ [cm^{-1}]$	0.50 ± 0.03	0.35 ± 0.02	0.50 ± 0.02	0.592 ± 0.005
$q_0\ [nm^{-1}]$	0.208 ± 0.001	0.31 ± 0.02	0.359 ± 0.009	0.411 ± 0.005
$\xi\ [nm]$	13.0 ± 0.4	3.06 ± 0.04	2.95 ± 0.03	2.59 ± 0.02
m_2	1.7 ± 0.2	1.57 ± 0.03	1.62 ± 0.02	1.62 ± 0.02
$D\ [cm^{-1}]$	0.0544 ± 0.0002	0.0694 ± 0.0003	0.1361 ± 0.0004	0.1536 ± 0.0005

$C_{10}(PC_{10})_4$

	6.5%	**10.5%**	**19%**	**31%**
A	$(2 \pm 1) \times 10^{7}$	$(6 \pm 8) \times 10^{6}$	$(4 \pm 4) \times 10^{6}$	$(2 \pm 2) \times 10^{7}$
$R_{agg}\ [nm]$	$(4 \pm 3) \times 10^{7}$	$(7 \pm 10) \times 10^{6}$	$(4 \pm 5) \times 10^{6}$	$(1 \pm 2) \times 10^{7}$
s	1 ± 1	0.4 ± 0.1	0.3 ± 0.1	0.31 ± 0.07
$B\ [cm^{-1}]$	65 ± 9	144 ± 7	340 ± 20	288 ± 9
$\Xi\ [nm]$	23 ± 1	24.0 ± 0.3	26.0 ± 0.3	23.5 ± 0.1
m_1	3.89 ± 0.09	4.00	4.00	4.000 ± 0.002
$C\ [cm^{-1}]$	0.62 ± 0.01	0.5366 ± 0.0009	0.623 ± 0.001	2.429 ± 0.004
$q_0\ [nm^{-1}]$	0.228 ± 0.009	0.435 ± 0.002	0.577 ± 0.001	0.3037 ± 0.0006
$\xi\ [nm]$	2.54 ± 0.02	2.28 ± 0.01	2.33 ± 0.02	4.62 ± 0.01
m_2	1.88 ± 0.01	1.84 ± 0.01	1.739 ± 0.009	1.745 ± 0.003
$D\ [cm^{-1}]$	0.0713 ± 0.0002	0.1058 ± 0.0002	0.2126 ± 0.0004	0.2051 ± 0.0003

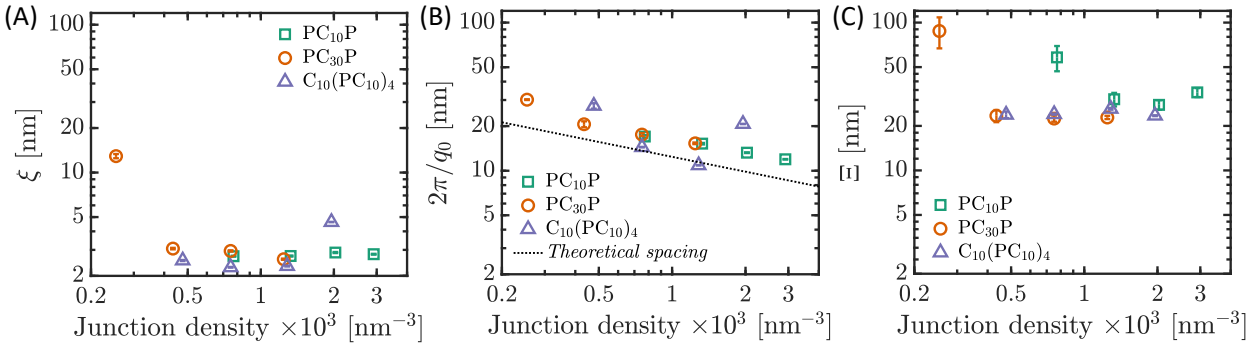

Figure S2. Structural length scales of all protein gels from fits of the combined SANS/USANS patterns to the double-correlation-length model (Equation 4 in the main text) as a function of junction density: (A) Correlation blob size ξ, (B) inter-junction spacing $2\pi/q_0$, and (C) large-scale correlation length Ξ. Error bars are standard deviations from 100 bootstrapped replicates of each combined scattering pattern. In Panel B the theoretical spacing is calculated assuming a random junction distribution as in an ideal gas, discussed in Section 7 of the Supplementary Information.

From the values of B obtained from fits to the double-correlation-length model (see Equation 5b in the main text) and the calculated scattering length densities of the protein and deuterated buffer, the root-mean-square fractional static density fluctuation associated with the large-scale correlation length Ξ can be estimated for each gel. The scattering amplitude B in Equation 5b associated with fluctuations on the length scale Ξ can be approximated as[2]

$$B \approx (\rho_{protein} - \rho_{buffer})^2 \left(\frac{\langle \delta c^2 \rangle}{c^2}\right) \Xi^3 \#(S1)$$

where ρ_i is the coherent neutron scattering length density of species i and $\langle \delta c^2 \rangle / c^2$ is the fractional mean-square concentration fluctuation associated with the length scale Ξ. The scattering length densities of the protein and buffer components were calculated from their chemical composition using bound neutron scattering lengths of common atoms tabulated by NIST.[3] The protein mass density was approximated as 1.3 g/mL, as in prior work,[4] and the buffer was approximated as pure D_2O, which has a mass density of 1.11 g/mL. The scattering length densities computed using the NIST calculator were $\rho_{protein} = 1.9 \times 10^{14}\, m^{-2}$ for all proteins and $\rho_{buffer} = 6.39 \times 10^{14}\, m^{-2}$ for the

buffer, as summarized in **Table S2**. Supplying these scattering length densities and best-fit length scales Ξ into Eq. S1 results in calculated root-mean-square static density fluctuations ranging from $\langle \delta c^2 \rangle^{\frac{1}{2}} / c = 0.01 - 0.12$ for all the gels, depending on the concentration, as shown in **Figure S3**.

Table S2. Coherent neutron scattering length densities of materials calculated from their chemical composition and density using atomic bound scattering lengths tabulated by NIST.

Material	**Chemical composition**	**Density** (g/mL)	**Scattering length density** ($\times 10^{14}\, m^{-2}$)
$PC_{10}P$	$C_{854}H_{1366}N_{272}O_{301}S_7$	1.3	1.9
$PC_{30}P$	$C_{1508}H_{2366}N_{488}O_{555}S_{11}$	1.3	1.9
$C_{10}(PC_{10})_4$	$C_{2595}H_{4077}N_{829}O_{959}S_{19}$	1.3	1.9
Buffer	D_2O	1.11	6.39

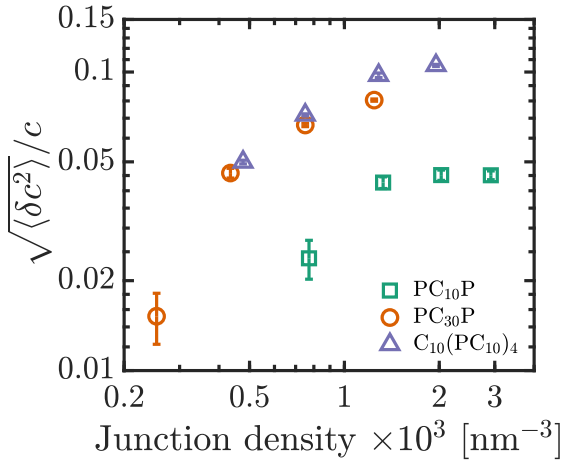

Figure S3. Root-mean-square static density fluctuation associated with the large-scale correlation length Ξ in all protein gels as a function of junction density.

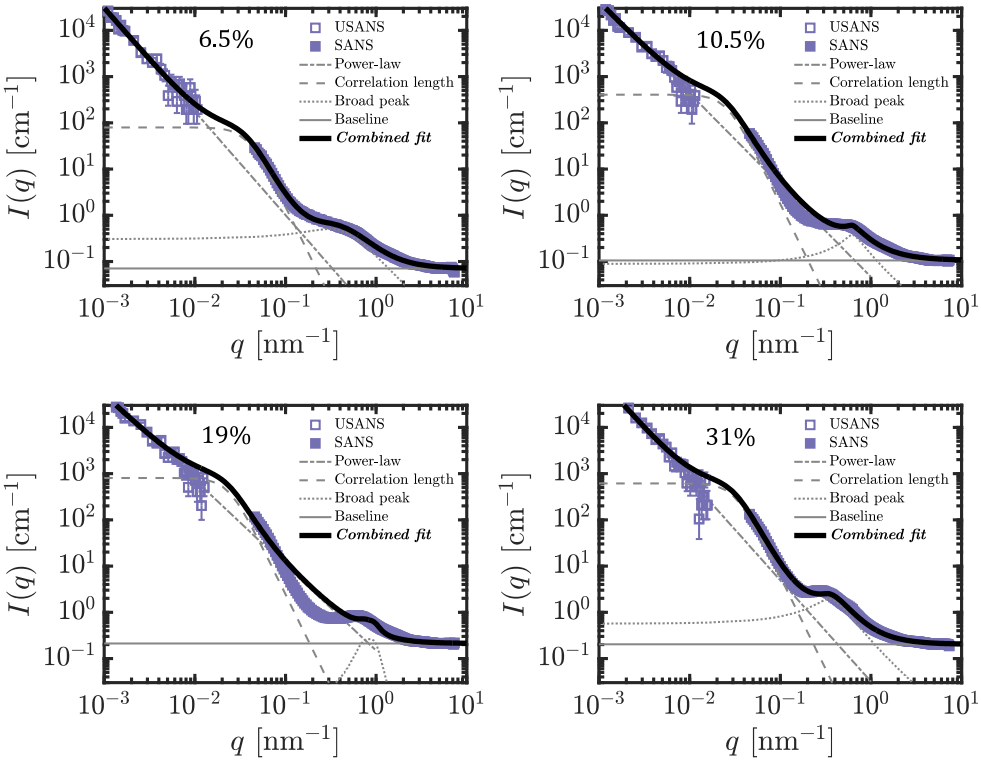

Figure S4. Fits of the neutron scattering data for the $C_{10}(PC_{10})_4$ gels to the double-correlation-length model using a power-law term for the low-q region, which does not decay fast enough to allow fitting of the higher-q regions.

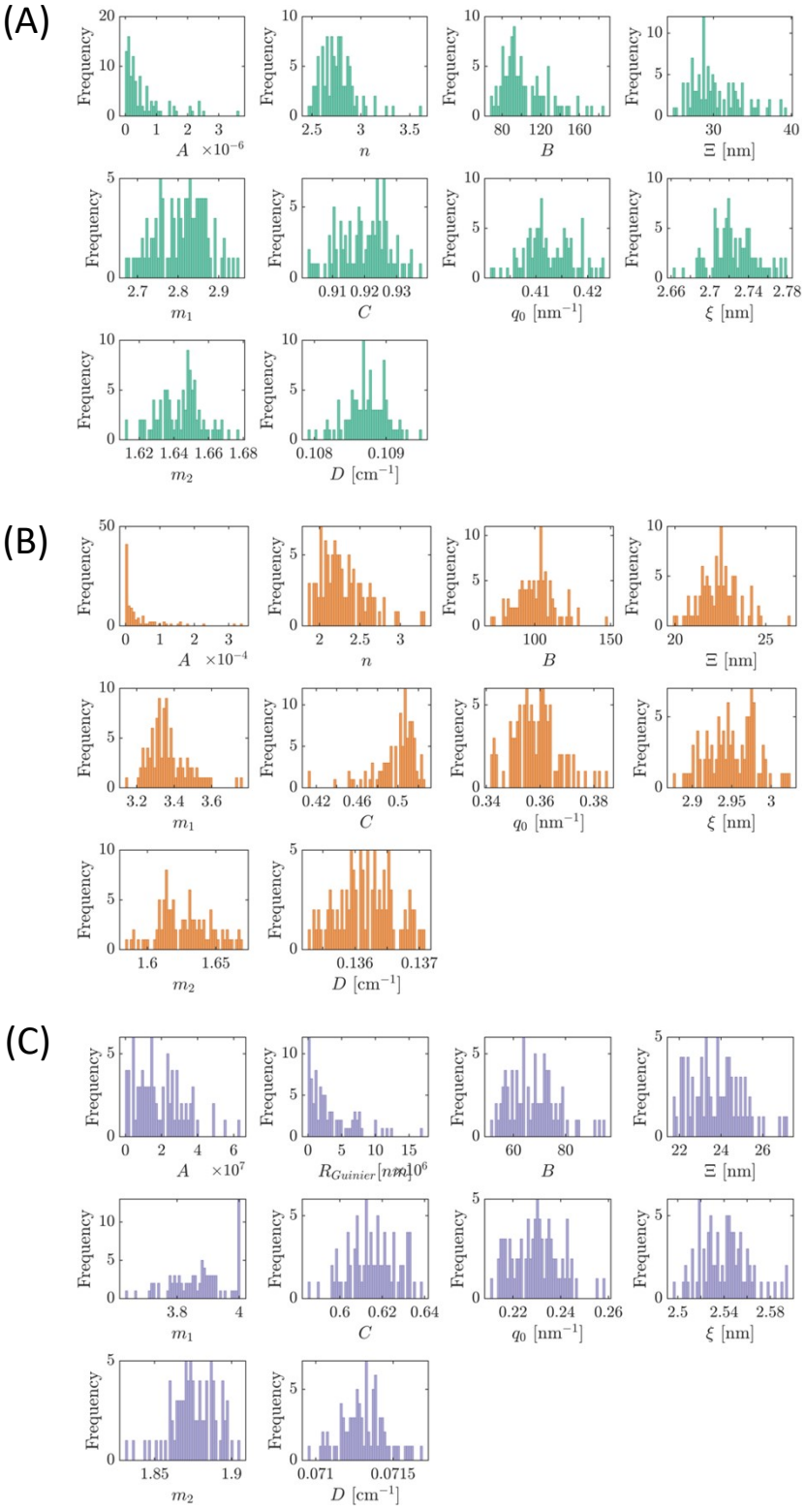

Figure S5. Representative histograms for fit parameters from 100 bootstrapped replicates of the combined SANS/USANS patterns for (A) $PC_{10}P$, 12.5%, (B) $PC_{30}P$, 12.5%, and (C) $C_{10}(PC_{10})_4$, 6.5% fit to the double-correlation-length model (Equation 4).

3. Frequency sweeps of protein gels

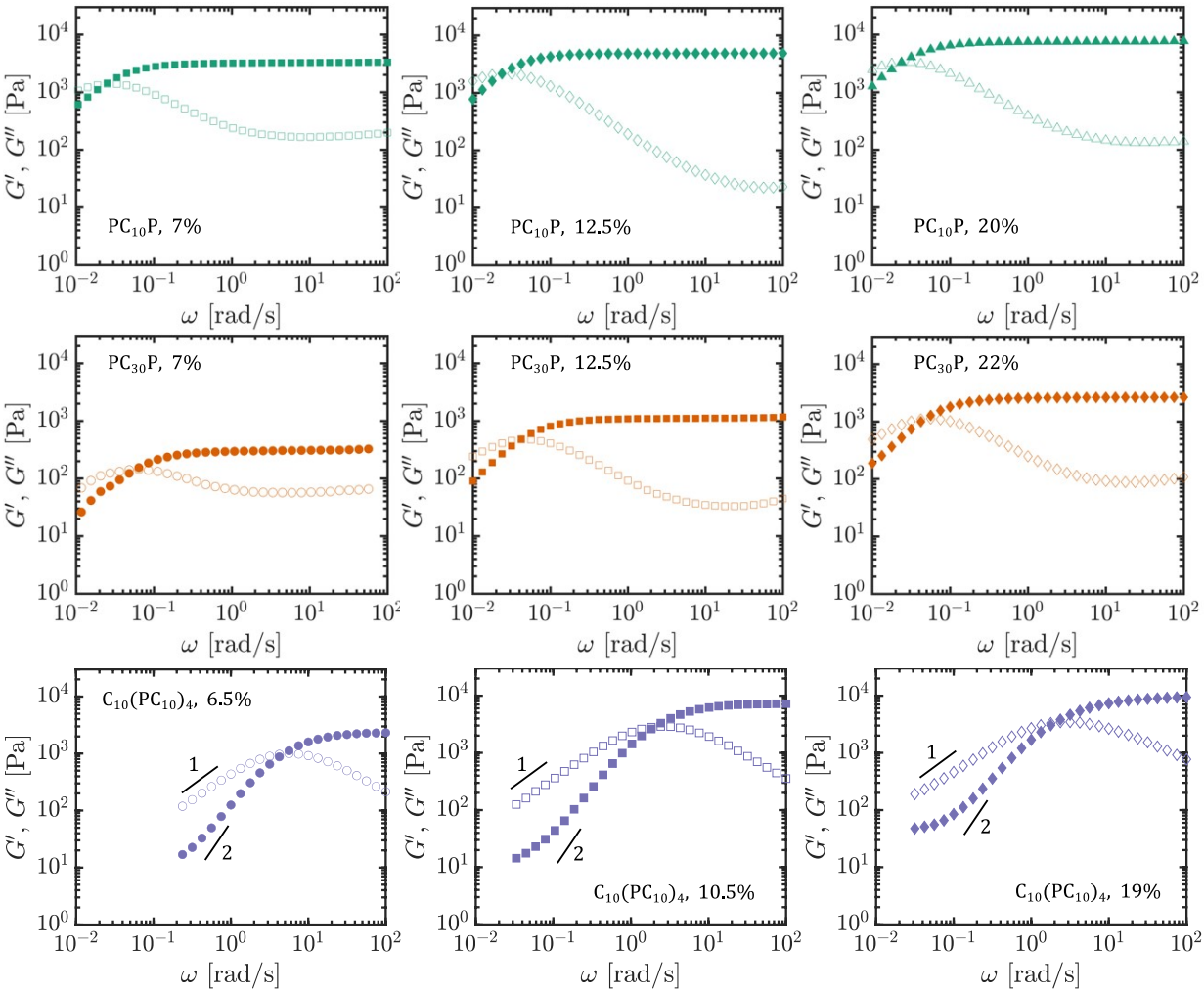

Figure S6. Frequency sweeps of all protein gels of various concentrations obtained at 35 ˚C with a 2% strain (within the linear viscoelastic regime).

4. Two-state model for anomalous diffusive behavior

A. Model description

Forced Rayleigh scattering data for self-diffusion and tracer diffusion of associative proteins were quantitatively analyzed using a previously developed two-state reaction-diffusion

model. Full details of the model and its predicted diffusion regimes are provided in Refs. [4,5] and summarized in this section. Briefly, the model postulates that associative polymers can exist in two diffusive states A and F with distinct diffusivities D_{slow} and D_{fast}, respectively. These states may correspond to an associated state A, where at least one sticker of a molecule is bound to the network, and a free state F, where the molecule is completely detached from the network (also termed hopping). However, the two-state model does not specify the exact molecular origin for each self-diffusive state. The diffusive species are assumed to interconvert according to the dynamic equilibrium

$$A \rightleftharpoons F \#(S2)$$

where the forward and reverse interconversion rates are governed by pseudo-first-order rate constants k_{off} and k_{on}, respectively, which are related by the pseudo-first-order effective equilibrium constant $\kappa_{eq} = k_{on}/k_{off}$. Conservation of mass implies the following coupled equations governing the reaction and diffusion dynamics of each species (in each dimension):

$$\frac{\partial[A]}{\partial t} = D_{slow}\frac{\partial^2[A]}{\partial x^2} + k_{on}[F] - k_{off}[A] \#(S3a)$$

$$\frac{\partial[F]}{\partial t} = D_{fast}\frac{\partial^2[F]}{\partial x^2} - k_{on}[F] + k_{off}[A] \#(S3b)$$

This coupled system can be solved by Fourier transform[4] to obtain an analytical relationship between the self-diffusion relaxation time $\langle\tau\rangle$ and grating spacing $d^2/4\pi^2$ of the FRS experiment, as shown graphically in **Figure S7**A.

For diffusion of a single-sticker tracer through the associative protein gels, the two diffusive states hypothesized by the model are expected to correspond exactly to its associated and free molecular states, respectively. This allows the forward and reverse interconversion rates in Eq. S3 to be expressed as *intrinsic* single-sticker association and dissociation rate constants,

denoted k_A^* and k_D, respectively, rather than k_{on} and k_{off}. Here, k_A^* is a pseudo-first-order forward rate constant related to the true second-order rate constant via $k_A^* = k_A F_{eq}$, where F_{eq} is the equilibrium density of free binding sites. Similarly, the pseudo-first-order equilibrium constant for single-sticker association is defined as $K_{eq}^* = F_{eq} K_{eq}$, where $K_{eq} = k_A/k_D$ is the second-order equilibrium constant for coiled-coil association. Note that the single-sticker equilibrium constants K_{eq} and K_{eq}^* are distinct from the two-state model parameter $\kappa_{eq} = k_{on}/k_{off}$, which describes the interconversion between the two apparent self-diffusive species rather than individual stickers. Furthermore, the best-fit diffusivity of the slow (i.e., associated) state of the single-sticker tracer is found to be $D_{slow} = 0$ for all tracer diffusion data, which results in a plateau in the relaxation time down to the smallest length scales. The predicted diffusive regimes for single-sticker tracer diffusion from the two-state model are graphically illustrated in **Figure S7**B.

B. Model predictions

Examining the predicted regimes for self- and tracer diffusion in **Figure S7** allows various relevant length and time scales governing their dynamics to be quantitatively inferred. For self-diffusion (**Figure S7**A), the two-state model predicts a small-length-scale Fickian regime with diffusivity governed by the slow mode, D_{slow}, followed by an apparent superdiffusive regime with an inflection point at the transition timescale $\tau_{off} = k_{off}^{-1}$, followed by a large-length-scale Fickian regime with terminal diffusivity governed by the diffusivity of the fast mode, D_{fast}, weighted by its population (Eq. 6 of the main text). The length scales governing the transition between the slow and fast diffusive modes, $d_{slow}^2/4\pi^2$ and $d_{fast}^2/4\pi^2$, can also be calculated from the intersection between the small- and large-length-scale Fickian regimes and the interconversion timescale k_{off}^{-1} (Eq. 7 of the main text).

For single-sticker tracer diffusion, the two-state model predicts a plateau on small length scales with relaxation time equal to the sticker dissociation time, $\tau_D = k_D^{-1}$, followed by terminal Fickian diffusion with diffusivity governed by the diffusivity of the free molecule, D_{free}, weighted by the fraction of free molecules. The length scale governing the transition to terminal Fickian diffusion, $d_{hop,tracer}^2/4\pi^2$, can be calculated from the intersection between the terminal Fickian regime and the dissociation timescale k_D^{-1}.

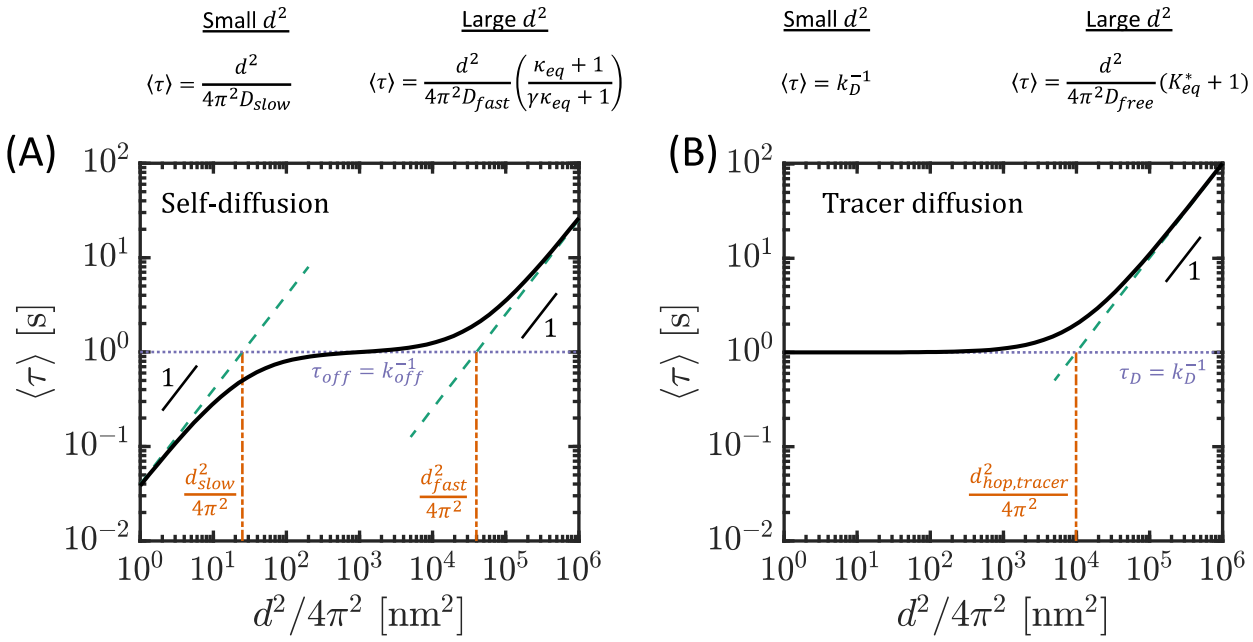

Figure S7. Representative predictions of the two-state model for (A) self-diffusion and (B) tracer diffusion. Parameters used for these example plots are (A) $k_{on} = 100\ s^{-1}$, $k_{off} = 1\ s^{-1}$, $D_{slow} = 25\ nm^2 s^{-1}$, $D_{fast} = 4 \times 10^6\ nm^2 s^{-1}$ and (B) $k_{on} = 100\ s^{-1}$, $k_{off} = 1\ s^{-1}$, and $D_{free} = 10^6\ nm^2 s^{-1}$. Analytical expressions for the relationship between $\langle\tau\rangle$ and $d^2/4\pi^2$ for the small- and large-length-scale Fickian regimes are provided above each plot, where by definition $\gamma = D_{slow}/D_{fast}$ and $\kappa = k_{on}/k_{off}$.

5. Method to calculate mean-first-passage dissociation times

Mean-first-passage times for the conversion from the fully bonded state to the fully unbonded state for a chain with S stickers were calculated by assuming that each sticker undergoes

stochastic association and dissociation reactions with pseudo-first-order rate constants k_A^* and k_D, respectively, and that each sticker's dynamics are uncorrelated from the others. The pseudo-first-order equilibrium constant is defined as $K_{eq}^* = k_A^*/k_D$. The time evolution of the chain's bonding configuration (i.e., its number of bonded stickers $n \in [0,S]$) is analogous to a random walk on a one-dimensional lattice with sites corresponding to the number of bonded stickers, n, and transition probabilities given by the rate constants k_A^* and k_D multiplied by the degeneracy of each transition, as shown in **Figure S8**.

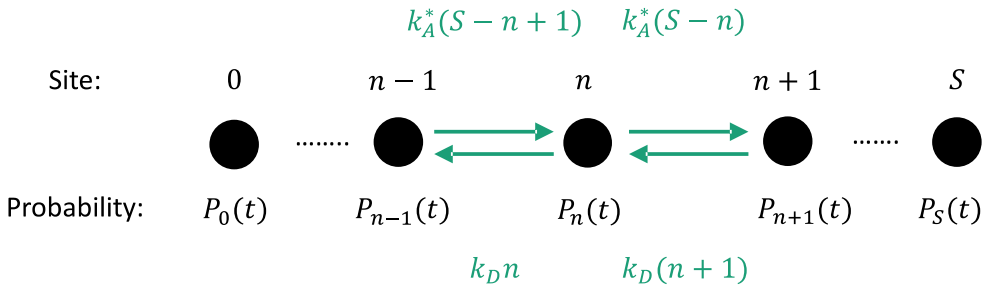

Figure S8. Schematic of a random walk on a one-dimensional lattice with sites corresponding to $n \in [0,S]$ bonded stickers with transition probabilities given by the rate constants k_A^* and k_D multiplied by their respective degeneracies (assuming identical average dynamics of each sticker).

The time evolution of this system is governed by the following coupled equations, where $P_n(t)$ is the probability of occupancy of site n:

$$\frac{dP_0(t)}{dt} = k_D P_1(t) \#(S4a)$$

$$\frac{dP_{n\in[1,S-1]}(t)}{dt} = -k_A^*(S-n)P_n(t) - k_D n P_n(t) + k_A^*(S-n+1)P_{n-1}(t) + k_D(n+1)P_{n+1}(t) \#(S4b)$$

$$\frac{dP_S(t)}{dt} = -k_D S P_s(t) + k_A^* P_{S-1}(t) \#(S4c)$$

Equation S4 can be expressed in matrix-vector form:

$$\dot{P}(t) = WP(t) \#(S5)$$

where $P(t)$ is an $S+1$ element vector of the probabilities of occupying states $n \in [0,S]$ and W is an $(S+1) \times (S+1)$ element matrix containing the transition probabilities corresponding to Equation S4. Thus, for $n \in [1,S-1]$, the elements of W are given by

$$W_{n,n-1} = k_A^*(S-n+1) \#(S6a)$$

$$W_{n,n} = -k_A^*(S-n) - k_D n \#(S6b)$$

$$W_{n,n+1} = k_D(n+1) \#(S6c)$$

To solve for the mean-first-passage time for conversion from the $n = S$ to the $n = 0$ state, an absorptive boundary condition is applied to the $n = 0$ site, such that for all n

$$W_{n,0} = 0 \#(S6d)$$

which is also reflected in Equation S4a. This ensures that once the chain has reached the fully dissociated state ($n = 0$) it stays there for all later times.

The initial condition for the system is designated to be the fully bonded state, i.e., $P_S(0) = 1$ and $P_{n<S}(0) = 0$, such that

$$P(0) = \begin{pmatrix} 0 \\ 0 \\ \dots \\ 1 \end{pmatrix} \#(S7)$$

The initial value problem given by Equations S5 and S7 is then solved by the matrix exponential:

$$P(t) = \exp(Wt)P(0) \#(S8)$$

The survival probability for this random walk, i.e., the probability that the chain still has at least one bonded sticker, is given by

$$S(t) = \sum_{n=1}^{S} P_n(t) \#(S9)$$

and the mean-first-passage dissociation time is given by the time-averaged survival probability,

$$\tau_{MFP} = \int_0^\infty S(t)dt \#(S10)$$

To calculate the normalized dissociation times, the mean-first-passage times are divided by the single-sticker dissociation time given by $\tau_D = k_D^{-1}$. Normalized mean-first-passage dissociation times for various values of S and K_{eq}^* are shown in **Figure S9**.

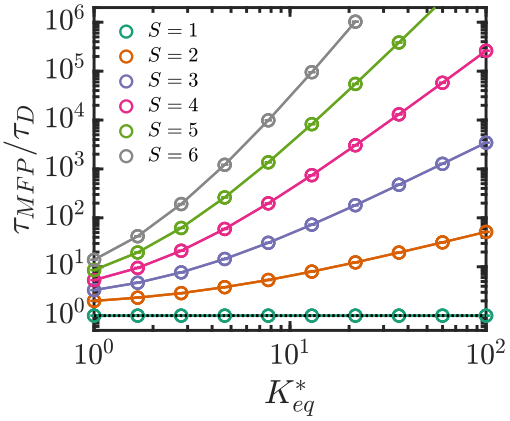

Figure S9. Normalized mean-first-passage dissociation times as a function of K_{eq}^* for various values of S.

6. Other supplementary figures referenced in the main text

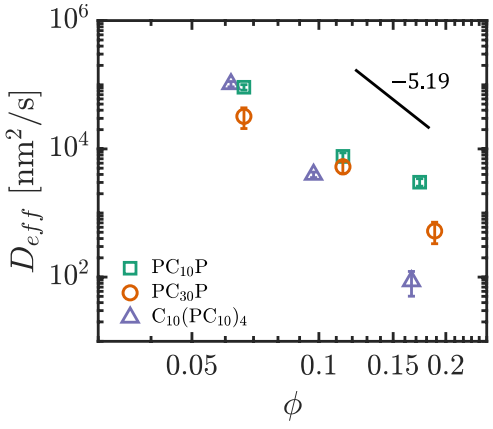

Figure S10. Terminal self-diffusion coefficient, D_{eff}, for each protein gel as a function of volume fraction, ϕ, at 35 ˚C.

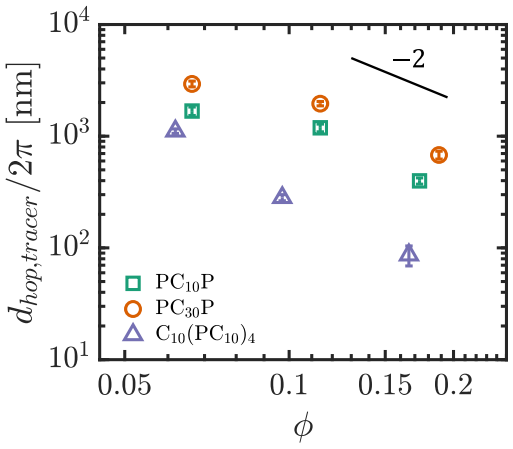

Figure S11. Hopping distance for the single-sticker tracer, calculated from the two-state model fit parameters via Equation 7 in the main text, for each protein gel as a function of volume fraction.

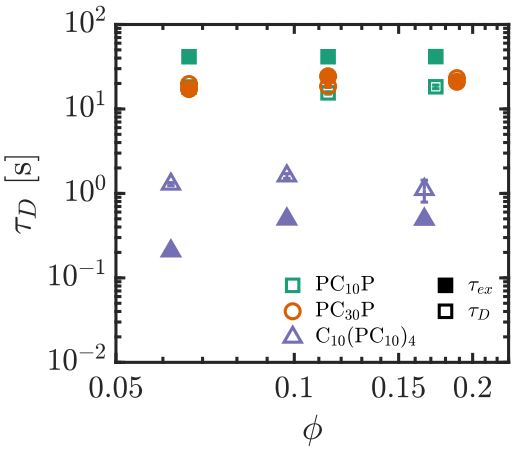

Figure S12. Comparison of single-sticker dissociation time, τ_D, measured from tracer diffusion experiments and network relaxation time, τ_{ex}, measured by shear rheology for all protein gels as a function of concentration.

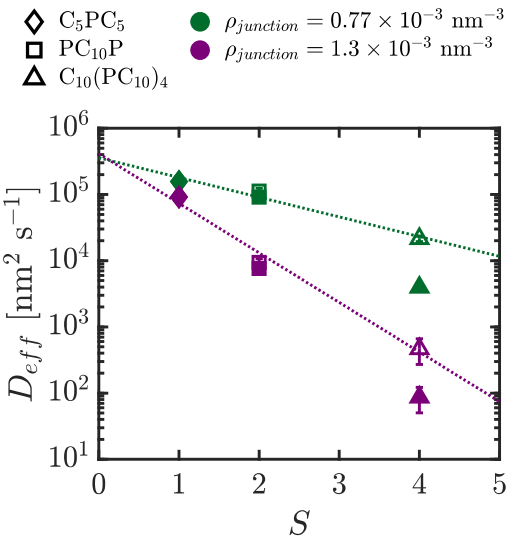

Figure S13. Comparison of the terminal diffusion coefficients as a function of number of stickers per chain, both corrected for changes in viscosity and molecular weight (open symbols) and uncorrected (closed symbols).

7. Calculation of theoretical junction spacing in the gel

Assuming a random distribution of network junctions (as in an ideal gas), the average distance between junctions can be estimated as the diameter of a sphere with volume equal to the inverse number density of junctions in the gel. The number density of the junctions in the gel, $n_{junction}$, is determined from the total protein concentration, molar mass, number of coiled-coil domains per chain, and pentameric junction aggregation number. The average distance between junctions can then be calculated as

$$d_{junction} = 2\left(\frac{3}{4\pi n_{junction}}\right)^{\frac{1}{3}} \#(S11)$$

8. References

1 A. Rao, H. Yao and B. D. Olsen, *Phys. Rev. Res.*, 2020, **2**, 043369.
2 S. Seiffert, *Prog. Polym. Sci.*, 2017, **66**, 1–21.
3 P. Kienzle, Neutron activation and scattering calculator, https://www.ncnr.nist.gov/resources/activation/, (accessed 28 November 2022).
4 S. Tang, M. Wang and B. D. Olsen, *J. Am. Chem. Soc.*, 2015, **137**, 3946–3957.
5 S. Tang and B. D. Olsen, *Macromolecules*, 2016, **49**, 9163–9175.